ELSEVIER

Surface Science 306 (1994) 367–380

surface science

# Polycrystalline surface properties from spherical crystallites: Ag, Au, Cu and Pt

S. Swaminarayan *, R. Najafabadi, D.J. Srolovitz

*Department of Materials Science and Engineering, University of Michigan, Ann Arbor, MI 48109-2136, USA*

(Received 23 August 1993; accepted for publication 9 November 1993)

**Abstract**

We have performed a series of atomistic simulations of nearly spherical, crystalline (fcc) clusters of Ag, Au, Cu and Pt as a function of temperature and cluster size. Since both a spherical cluster and a random polycrystal expose all possible surfaces equally, this provides a plausible approach for determining the surface properties of random (non-textured) polycrystalline metals and to find a simple expression to relate these average surface properties to the oft calculated properties of high symmetry/low index surfaces. Atomic clusters with radii greater than approximately $4a_0$ yield cluster average surface energies and surface stresses are within a few percent of those obtained from very large clusters. The variation of the cluster average surface properties with cluster size is dominated by a geometrical effect associated with the discrete spacing between atomic planes and that the differences associated with differences in the atomic bonding between different elements is small, at least for the four elements considered herein. Comparison of the cluster average surface free energy with those of the more commonly studied high symmetry flat {100}, {110}, and the {111} surfaces suggest two useful approximations for the average surface free energy: (1) equating it to the surface free energy of a {110} surface and (2) using a linear fit to the {100}, {110}, and the {111} surface free energies. Conversely, the first approximation provides an accurate estimate of the {110} surface energy from experimentally measured polycrystalline surface energies.

## 1. Introduction

Most crystalline materials used in technologically interesting applications are polycrystallites rather than single crystals. As a consequence, the exposed surfaces of these materials represent all possible crystallographic surface orientations. Unfortunately, the majority of surface studies have focused on the properties of high symmetry, low index surfaces. The question of how to extrapolate from the properties of a few high symmetry surfaces to the average properties of a random, polycrystalline material remains open. The focus of the present paper is the determination and analysis of average surface thermodynamic properties.

It is not feasible to directly determine average surface properties of a polycrystalline sample via atomistic simulations due to the large number of atoms necessary for such a study. As an alternative, we examine the average surface properties of spherical clusters of atoms. Since both a sphere and a random (untextured) polycrystalline solid

* Corresponding author. Fax: +1 (313) 763-4788.


*SSDI* 0039-6028(93)E1000-P

expose all possible surfaces, we expect that the average surface properties of a sphere will provide a good approximation to the average surface properties of a random polycrystal. The average surface properties of textured polycrystals are, however, not accurately represented by such spherical averages. Simulations were performed as a function of spherical cluster size in order to isolate the effect of finite cluster size. Clusters of metal atoms are also of interest in catalysis since many practical catalysts are in the form of small (10–100 Å) metal particles.

The two surface properties that we focus on in the present study are surface free energy and surface stress. Although the terms surface free energy and surface tension (or stress) are often used interchangeably, the surface free energy and surface stress are quite distinct for a solid. The surface stress $\tau_{\alpha\beta}$ is the variation of the total surface free energy with respect to strain $\epsilon_{\alpha\beta}$:

$$\tau_{\alpha\beta} = \gamma\delta_{\alpha\beta} + \frac{\partial\gamma}{\partial\epsilon_{\alpha\beta}}, \tag{1}$$

where $\gamma$ is the surface free energy per unit area, $\delta_{\alpha\beta}$ is the Kronecker delta function and $\alpha$ and $\beta$ are two orthogonal directions in the surface. In a liquid, however, the second term in Eq. (1) is identically zero and the surface stress and surface energy are equivalent. This is because when a liquid is strained at constant temperature, additional atoms move into the surface positions and the structure of the surface remains unchanged.

It is the surface stress that is responsible for the internal stresses and changes in lattice constants of small clusters. As an example, consider a spherical, elastically isotropic crystal of radius $R$ whose interior, due to the surface stress, is under compression. If we make an imaginary cut through the origin of the sphere, and perform a force balance in the $z$-direction then we can show that in the limit that the thickness of the surface goes to zero, the pressure $P$ resulting from a finite surface stress $\tau$ is given by

$$P = -2\tau/R. \tag{2}$$

In deriving Eq. (2), $\tau$ is the average tangential surface stress, where the average is taken over both the entire surface area of the cluster and over the $\theta\theta$ and $\phi\phi$ components of the surface stress tensor. The stress state within this sphere of zero surface thickness would be purely hydrostatic and would be uniform throughout the sphere, except right at the surface. Experiments [1] have shown that the change in lattice parameter is inversely proportional to particle size, in agreement with Eq. (2).

In the present paper, we determine the average surface free energy and surface stress of spherical clusters of Ag, Au, Cu and Pt atoms as a function of cluster size and temperature. In addition, we independently measure the pressure internal to the cluster and the surface stress in order to validate Eq. (2). We also investigate the variation of internal stress within the cluster to determine the effective width of the surface.

## 2. Simulation method

As described above, the simulations were performed on spherical clusters of atoms. Since these clusters were carved out of infinite fcc crystals (i.e., all atoms within a distance less than or equal to $R$ of a central atom are included within the cluster), the "spherical" clusters exhibit small facets. This is not unreasonable, however, since all high index surfaces are describable in terms of steps and terraces. As the cluster radius $R$ is increased, these clusters become increasingly better approximations to true spheres. It is in the limit that $R \to \infty$, the surface properties of the cluster represent true spherical averages. Several simulations were also performed for flat surfaces bounding semi-infinite crystals, in order to compare with the spherical cluster results. These simulation were performed using the free energy minimization method, as in our previous grain boundary studies [2].

### 2.1. The free energy simulation method

At finite temperatures, the central thermodynamic property of a cluster is its free energy. In pure materials, the free energy, $A$, has two main contributions: a static lattice energy $A_0$ and a term attributable to atomic vibrations $A_v$. The

static lattice energy is simply the energy of the atomic structure in which each atom is frozen at its average position. In the present study, we model the static lattice energy in terms of the widely applied embedded atom method (EAM) interatomic potentials [3]. These potentials have been shown to yield excellent agreement with a wide variety of experimental data.

At sufficiently low temperatures (i.e., up to about nine tenths of the melting point [2,4]), the motions of the atoms in a solid are nearly harmonic. We can simplify this harmonic approximation further by neglecting the terms that couple atoms together. The vibrational contribution to the Helmholtz free energy, $A_v$, is thus given by [2]

$$A_v = k_B T \sum_{i=1}^{N} \sum_{\beta=1}^{3} \ln\left[2 \sinh\left(\frac{\hbar\omega_\beta^i}{2k_B T}\right)\right], \tag{3}$$

where $N$ is the total number of atoms within the system, $k_B T$ is the thermal energy, $\hbar$ is Planck's constant and $\omega_\beta^i$ are the three vibrational frequencies associated with atom $i$. Under the assumptions of the local harmonic model [2,4], it is possible to determine the $\omega_\beta^i$ for a perfect crystal, by diagonalizing the local dynamical matrix for each particle $i$ within the unit cell. In the classical limit ($\hbar\omega \ll k_B T$), Eq. (3) simplifies to

$$A_v = 3k_B T \sum_{i=1}^{N} \ln\left(\frac{\hbar D_i^{1/6}}{k_B T}\right), \tag{4}$$

where $D_i = [\omega_{1i}\omega_{2i}\omega_{3i}]^2$ is the determinant of the local dynamical matrix of particle $i$. The equilibrium structure is obtained by minimizing the free energy with respect to the atomic coordinates of the particles within the cluster. This minimization is accomplished using the conjugate gradient method with the convergence criterion chosen such that the maximum pseudo-force ($-\partial A/\partial \boldsymbol{r}^i$) on any particle did not exceed $1 \times 10^{-5}$ eV/Å for the zero temperature simulations and $1 \times 10^{-4}$ eV/Å for the finite temperature simulations. A more detailed description of the free energy minimization method may be found in Ref. [2]. Previous studies have shown that this method yields accurate free energies for grain boundaries and point defects [2,4,5].

Although small atomic clusters often show faceting and can exhibit phases which are different from those seen in equilibrium bulk phases, the present study does not examine either of these two aspects of the structure of small clusters. In fact, the present simulation procedure was chosen such that the clusters represent the average surface properties of bulk crystal as well as possible.

### 2.2. Surface energy and stresses

The surface free energy $\gamma$ was determined as the difference between the free energy of the cluster of atoms and that of the same number of atoms in a perfect crystal at the same temperature and stress state as in the center of the cluster and divided by the surface area of the cluster ($4\pi R^2$). The bulk stresses $\sigma_{\alpha\beta}$ within the cluster may be written as

$$\sigma_{\alpha\beta}^i = -\frac{1}{\Omega^i} \sum_{k \neq i} F_\alpha^{ki} r_\beta^{ki}, \tag{5}$$

where $\Omega^i$ is the atomic volume associated with atom $i$ and $r_\beta^{ki}$ is the $\beta$ component of the vector connecting atoms $k$ and $i$. $F_\alpha^{ki} = -\partial A/\partial r_\alpha^{ki}$ is the pseudo-force on atom $i$ associated with the displacement of atom $k$ in the $\alpha$-direction, where $A$ is the free energy of the cluster.

A method for the determination of surface stresses of flat surfaces, where a unit cell can be defined, has been proposed by Ackland and Finnis [6]. The surface stress tensor is written as a sum over all of the atoms $i$ of the lattice

$$\tau_{\alpha\beta} = \sum_{i=1}^{N} A_c^{-1} \frac{\partial u_i}{\partial \epsilon_{\alpha\beta}} = -A_c^{-1} \sum_{i=1}^{N} \sum_{k \neq i} r_\beta^{ki} F_\alpha^{ki}, \tag{6}$$

where $\epsilon_{\alpha\beta}$ are the homogeneous strains within the plane of the surface, $A_c$ is the surface area of the unit cell, $u_i$ is the energy associated with atom $i$ within the unit cell. The summation over $k$ includes all the sites within the unit cell.

For the spherical clusters, there is no readily identifiable unit cell and no simple method for identifying surface atoms. Therefore, an alternative procedure was developed in order to avoid these difficulties. The surface stress is the deriva-

tive of the total surface free energy with respect to the homogeneous surface strain $\epsilon_\alpha$: $\tau_{\alpha\beta} = (1/A_c)\partial(\gamma A_c)/\partial\epsilon_{\alpha\beta}$. For the clusters, this becomes

$$\tau_{\alpha\beta} = A_c^{-1} \sum_{i=1}^{N} \sum_{k \neq i} r_\beta^{ki} F_\alpha^{ki} - \frac{PR}{3}\delta_{\alpha\beta}, \qquad (7)$$

where the summations are evaluated over all atoms in the system and the second term accounts for the stressed reference state. An explicit expression for the surface stress, derived for the embedded atom method (EAM) class of potential is given in the Appendix.

### 2.3. Implementation of symmetry

The present study focuses on a series of face centered cubic metals. Since the crystal structure of the clusters have cubic symmetry, we can reduce the number of atoms needed for simulating the spherical cluster by employing some of the symmetries of this crystal structure. By making use of the reflections in the {100} planes (i.e., the four-fold symmetry), it is possible to generate all atomic positions within the spherical cluster simply by considering only those atoms within a single octant (assuming that the cluster is centered at the origin). The positions of the atoms in all other octants can be obtained by reflections in the {100} planes. Making use of this mirror symmetry operator, we simulated spherical clusters with $R \leqslant 15a_0$ on a workstation with 16 Mbytes of memory, where $a_0$ is the fcc lattice parameter at zero pressure. Without employing this four-fold symmetry, we were only able to examine spherical clusters with $R \leqslant 8a_0$. It is possible to increase the cluster size even further by making use of the reflections in the {110} planes, but this would result in an increase of only $2a_0$ in simulated cluster size (to $17a_0$) and hence was not implemented.

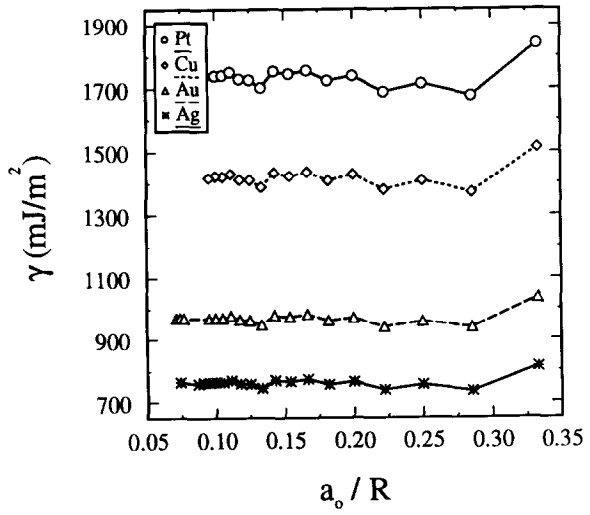


Fig. 1. Variation in surface free energy, $\gamma$, as a function of inverse cluster radius ($a_0/R$) at 0 K.

## 3. Results

### 3.1. Zero temperature

Spherical clusters of Ag, Au, Cu, and Pt with radii in the range $3a_0 \leqslant R \leqslant 14a_0$ were examined. In addition to the surface energy and surface stress, the following properties of the cluster interior were also examined: the lattice parameter at the center of the cluster ($a_{cent}$), the pressure at the center of the cluster ($P_{cent}$), and the overall stress state within each cluster.

Fig. 1 shows the variation of the surface energy of the clusters as a function of cluster size $R$ at $T = 0$ K. This figure shows that there is some variation in the average surface energy with cluster size $R$, with the largest variations occurring for small clusters. However, this variation in the average surface energy becomes small for clusters with radii larger than approximately $4a_0$ and very small for radii larger than $10a_0$. These results suggest that average surface energies have converged to within approximately 3% of the infinite radius results with clusters as small as $4a_0$ and to within 1% for $10a_0$ clusters. The large radii average surface energies for Ag is 765 mJ/m$^2$, for Au is 970 mJ/m$^2$, for Cu is 1422 mJ/m$^2$, and for Pt is 1742 mJ/m$^2$.

Comparison of the average surface energy results with experimental data [7] suggests errors of approximately 35%. This error is largely attributable to the empirical EAM interatomic po-

tentials. In fact, comparison of the energies of flat, high symmetry surfaces calculated based upon these same potentials [3] with experimentally measured surface energies of polycrystalline metals [7] show errors of 35–45%. This is much too large to be attributed to the difference between average and high symmetry surface energies, as discussed below. There is also considerable uncertainty in the experimentally determined surface energies as different researchers quote widely varying values [7]. The 0 K experimental data were obtained by extrapolating experimental data from high temperature using a linear correlation of the surface energy with the cohesive energy and an assumed surface entropy. Given this considerable uncertainty, the nature of the conclusions that can be drawn from the present study are limited to trends and correlations and the absolute values of the surface energies should be viewed as only semi-quantitative.

The overall shapes of the surface free energy versus $a_0/R$ curves for all four elements are very similar: i.e., a maximum at the smallest cluster size (largest value of $a_0/R$) and local minima at $a_0/R = 0.29$, 0.22 and 0.13. The similarity of these lattice parameter vs. sphere size curves suggests that the variation depends more on the discreteness of the lattice and crystal structure than on element type. We attempt to clarify this relation by normalizing all of the curves by the average surface energy of the $R = 10a_0$ cluster (see Fig. 2). This figure shows that most of the variation with cluster size is attributable to the different "shape" of the clusters as a function of cluster radius. The deviations from this "universal" form, attributable to the different element types is quite small and is not systematic.

Eq. (2) suggests that non-zero surface stresses will create a non-zero pressure within the cluster. The pressure at the center of the spherical cluster of atoms $P_{cent}$ is plotted in Fig. 3 as a function of inverse cluster size $a_0/R$ for $T = 0$ K. If the continuum elastic analysis is valid and the surface stress is independent of cluster size, then we should expect $P_{cent}$ to be directly proportional to $1/R$. Fig. 3 shows that except for the smallest atomic clusters ($R < 4a_0$), $P_{cent}$ is a linear function of the inverse sphere radius for all four

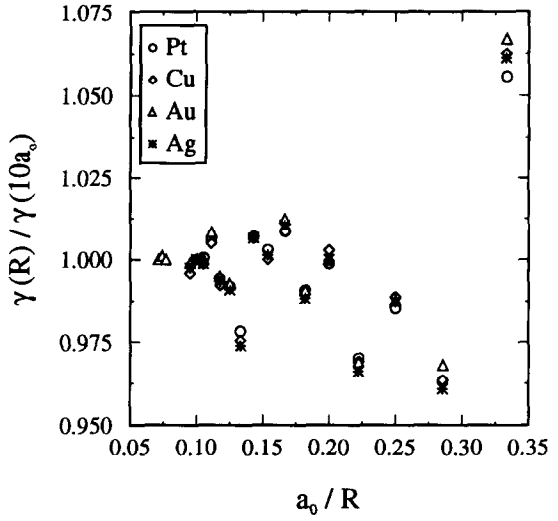


Fig. 2. Surface free energy for Ag, Au, Cu, and Pt (at 0 K) normalized using the value of energy at $10a_0$ for each element. All elements studied follow one "universal" curve when scaled.

elements examined and that the curves all extrapolate through $P_{cent} = 0$ in accordance with Eq. (2). The fluctuations about this straight line are attributable to lattice effects (as described above)

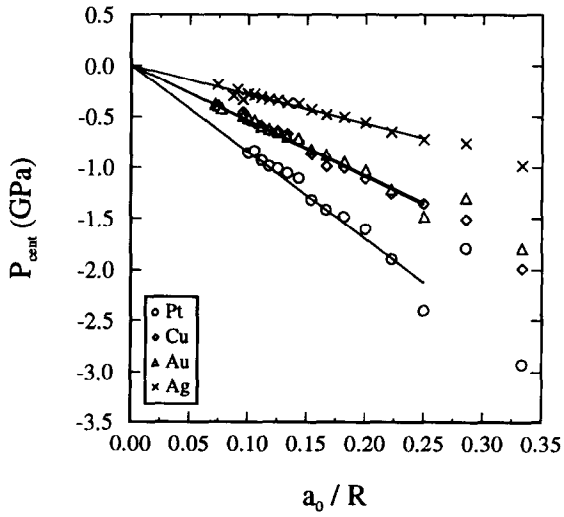


Fig. 3. Variation of the pressure at the center of clusters of various sizes as a function of scaled cluster radius ($a_0/R$) at 0 K. As expected, all the lines extrapolate to zero for clusters of infinite size.

which are manifested as small variations of the surface energy with cluster size. The fact that the $P_{cent}$ vs. $a_0/R$ curves all have negative slopes suggests that the average surface stress $\tau$ is tensile. The numerical value of the average surface stress is simply related to the slopes in Fig. 3. Associated with this internal pressure is a small change in lattice parameter at the center of the cluster $a_{cent}$, as shown in Fig. 4. Since the change in lattice parameter is directly proportional (within linear elasticity) to the pressure, it is not surprising that $a_{cent}$ is also a linear function of $1/R$. As $R$ gets large, $a_{cent}$ approaches the perfect crystal, zero pressure lattice parameter.

Fig. 5 shows the variation in the average bulk stress (averages taken over spherical shells) within a Au spherical cluster of radius $R = 13a_0$ as a function of distance from the center of the cluster. This variation is typical of all the clusters studied. All of the normal stresses are compressive, equal (i.e., the stress state is hydrostatic) and constant throughout the sphere until very close to the surface. The shear stresses are zero. These

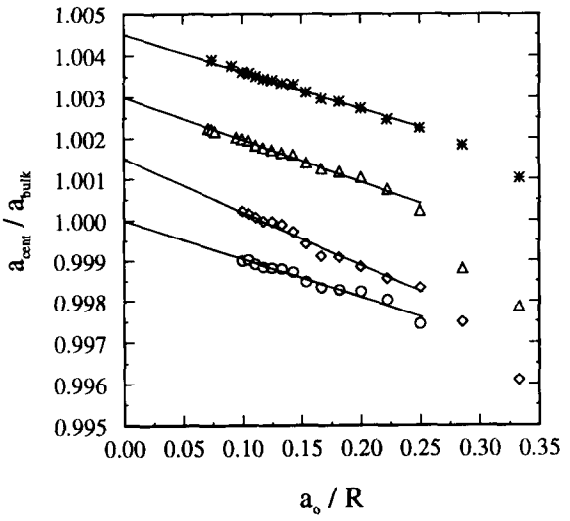


Fig. 4. Variation of lattice parameter at the center ($a_{cent}$) of the cluster as a function of scaled cluster size ($a_0/R$) at 0 K. The value of the lattice parameter extrapolates to the equilibrium perfect crystal value for all elements as the cluster size approaches infinity. The curves for Cu, Au and Ag have been shifted up by 0.0015, 0.003 and 0.0045 respectively, for clarity. (○) Pt, (◇) Cu, (△) Au, (*) Ag.

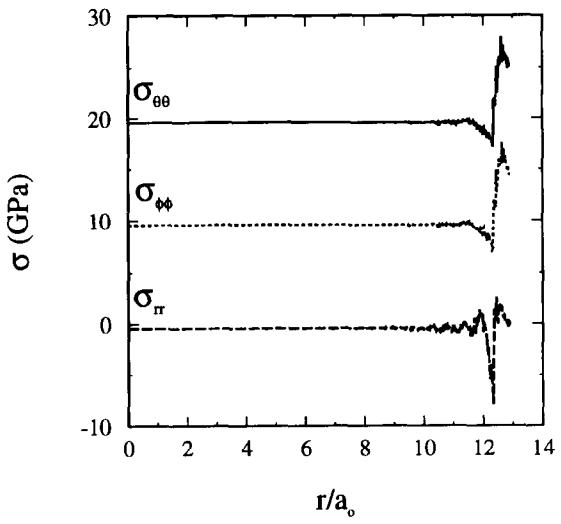


Fig. 5. Variation in the bulk stresses within a cluster of radius $R = 13a_0$. The curves for $\sigma_{\phi\phi}$ and $\sigma_{\theta\theta}$ have been shifted by 10 and 20 GPa respectively, for clarity.

are in agreement with a continuum elastic description of the stresses within a sphere which has a tensile (positive) surface stress. There is a distinct region near the surface that has a stress distribution much different from that of the bulk and can be associated with the presence of the surface. Although thickness of this surface layer is not well defined, the spatial variations of the all components of the stress suggest that $1.5a_0$ is a reasonable estimate of the surface "thickness". While part of this variation is attributable to surface relaxations, part of it is also associated with the fact that the unrelaxed surface is faceted. The stress state within this layer is complex. The radial stress $\sigma_{rr}$ must go to zero at the surface since the external pressure is zero (i.e., the zero normal traction elastic boundary condition). However, $\sigma_{rr}$ goes through several oscillations before it goes to zero. $\sigma_{rr}$ exhibits a very strong, compressive peak approximately $a_0/2$ below the surface. Approaching the surface from within, we find that $\sigma_{\theta\theta}$ becomes large and compressive (but not as compressive as $\sigma_{rr}$), then very large and tensile followed by a small drop at the surface of the sphere. By symmetry, we expect that $\sigma_{\theta\theta} = \sigma_{\phi\phi}$.

The generality of these results may be seen in Fig. 6, where we plot the variation of the average internal stress $\sigma_{rr}$ versus distance from the surface for clusters of several different radii. In all cases, the stresses are constant away from the surface layer and show the same general behavior near the surface. The thickness of the surface layer is found to be approximately independent of cluster size and is less than or equal to $1.5a_0$.

Fig. 7 shows the dependence of the average surface stress $\tau$ on the clusters size for gold and copper cluster determined using the method described in Eq. (7) and the Appendix. $\tau$ is evaluated as an average over the entire surface and over the two non-zero components of the normal surface stress $\tau_{\theta\theta}$ and $\tau_{\phi\phi}$. The average surface stress does not vary smoothly with cluster size. This is attributable to the discreteness of the crystal lattice, as in the case of the average surface energy. Comparison of Figs. 1 and 7 show that in the case of copper, the average surface stress is substantially smaller than the average surface energy, while in the gold case, the average surface stress is slightly larger than the average surface energy. Therefore, the second term in the surface stress in Eq. (1) is negative in one case (Cu) and positive in the other (Au), even though both metals are noble and have the same crystal structure. As discussed above, there are two methods for determining $\tau$: from Eq. (7) and from the slope of the internal pressure versus $1/R$ plots. These two methods yield surface stresses that are in good agreement with each other (within 2.5% for $R > 4a_0$). The slight discrepancies are again attributable to the discreteness of the lattice and the differences in the manner in which both measures of $\tau$ were summed.

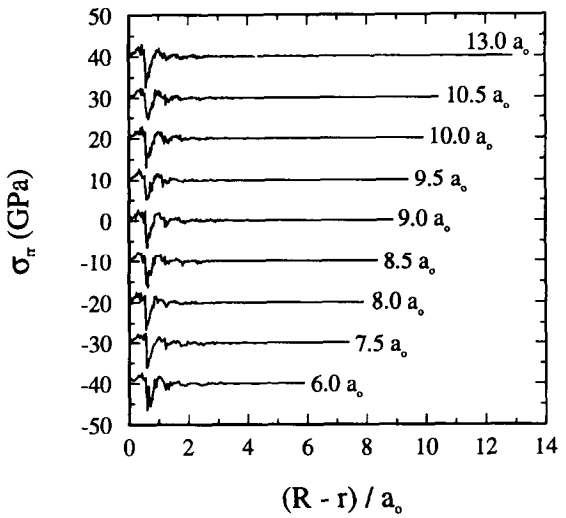


Fig. 6. Variation in the radial stress ($\sigma_{rr}$) as a function of scaled distance from the surface, $(R-r)/a_0$, for Au clusters of various sizes at 0 K. All curves (except for $9a_0$) have been shifted by integral multiples of 10 GPa respectively, for clarity.

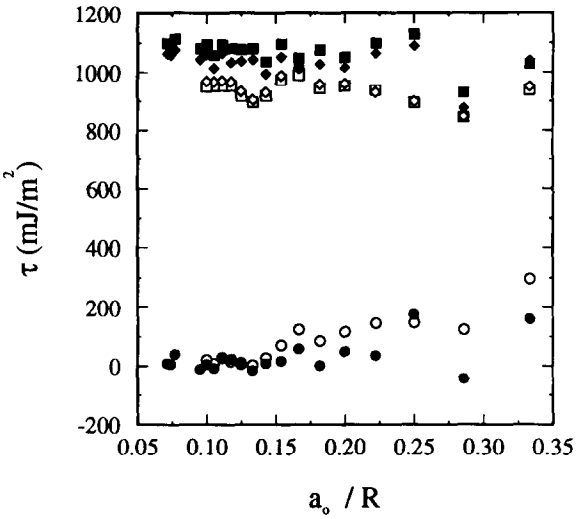


Fig. 7. Variation in surface stress for Au and Cu clusters as a function of inverse cluster size ($a_0/R$). The stress in the radial direction approaches zero as the cluster size increases and the tangential surface stress is equal to the value predicted using a continuum expression ($-PR/2$). (Cu: (□) $\tau_{\theta\theta}$, (◇) $-PR/2$, (○) $\tau_{rr}$. Au: (■) $\tau_{\theta\theta}$, (◆) $-PR/2$, (●) $\tau_{rr}$.)

### 3.2. Finite temperature

Au and Cu clusters of radii $6a_0$ and $10a_0$ were examined at 200, 400, 600, 800 and 1000 K. Fig. 8 shows the variation in surface free energy as a function of temperature for Au clusters of radii 6 and 10 lattice parameters. For reference, the finite temperature properties of perfect crystals of Au may be found in Ref. [2]. The average surface free energy is a nearly linear decreasing

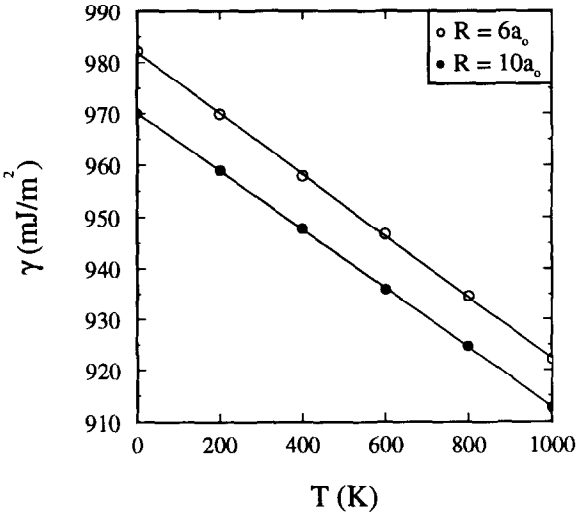


Fig. 8. Variation in the surface free energy, $\gamma$, of Au clusters of sizes $6a_0$ and $10a_0$ with temperature.

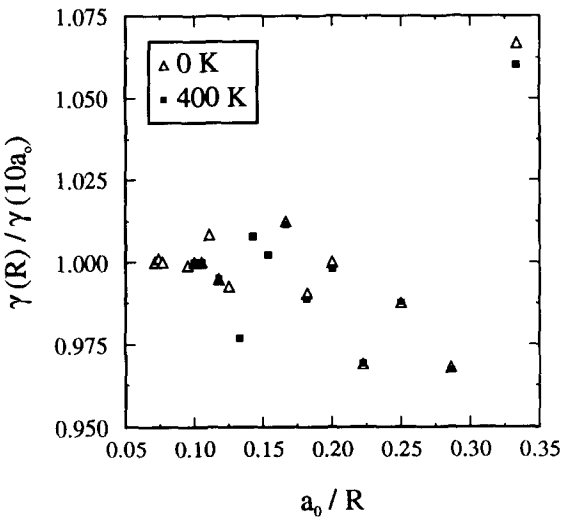


Fig. 9. Comparison of scaled surface free energy for Au clusters at 400 K with that of Au at 0 K.

function of temperature. This suggests that the average surface entropy is positive. A negative surface entropy does not violate the second law of thermodynamics (as long as the system entropy remains positive) since it is an excess quantity (i.e., the difference in the entropy of the system with and without a free surface). By fitting the surface free energy to a curve of the form $\gamma = H_s - TS_s$, we can quantify the temperature variation of the free energy and the values of the surface enthalpy and entropy (see Table 1). The surface entropy does not go to zero at $T = 0$ since the entropy was only fitted to high temperature data (the free energy model assumes that $\hbar\omega \ll k_B T$ and hence is not accurate below the Debye temperature). The variation in the average surface enthalpy and entropy with cluster radius (from $6a_0$ to $10a_0$) is only about 1% and 5%, respectively. Therefore, accurate estimates of the average surface thermodynamic properties may be obtained with small clusters.

Table 1
Average surface enthalpy and entropy of Au and Cu clusters of radii of 6 and $10a_0$ for $200 \leqslant T \leqslant 1000$ K

| | $H_s$ (mJ /m$^2$) | $S_s$ (mJ m$^2$ K) |
|---|---|---|
| Au: $6a_0$ | 982.06 | 0.05966 |
| $10a_0$ | 970.35 | 0.05733 |
| Cu: $6a_0$ | 1437.20 | 0.12601 |
| $10a_0$ | 1423.42 | 0.13347 |

In order to determine whether the finite temperature surface free energy data exhibited the same finite lattice size effects as did the 0 K data (Fig. 2), Au clusters of sizes ranging from $3a_0$ to $10a_0$ were studied at 400 K and compared with the 0 K data in Fig. 9. Clearly, the zero and finite temperature results are in good agreement. This is attributable to the fact that the entropy contribution to the average surface free energy is relatively small (less than a 5% change from 0 to 1000 K, see Fig. 8) and that the effects of thermal expansion have largely been scaled out by the sphere size normalization.

The variation in the average surface stress as a function of temperature for Au and Cu clusters of radius $6a_0$ at 200, 400, 600, 800 and 1000 K is shown in Fig. 10. The average surface stress $\tau$ decreases in a nearly linear manner with increasing temperature for both Au and Cu clusters. The average surface stress $\tau$ can be expanded in a Taylor series about $T = 0$: $\gamma = a + bT + cT^2$, where $a$ is the zero temperature surface stress (see above), $b = -0.06475$, $c = -1.3409 \times 10^{-4}$ for Au and $b = -0.1279$, $c = -7.6578 \times 10^{-5}$ for

Cu, where $T$ is in Kelvin and $\gamma$ is in mJ/m$^2$. The average surface stress varies by approximately 18% from 0 to 1000 K for both the Cu and Au clusters.

The variation of the lattice parameter at the center of an $R = 10a_0$ Cu cluster with temperature is shown in Fig. 11 along with data obtained for a perfect crystal of Cu at zero pressure. The thermal expansion coefficient, $\alpha = (1/a_0)(\partial a_0/\partial T)$, of the Cu perfect crystal (measured at $T = 0$) is $\alpha_p^{Cu} = 19.5 \times 10^{-6}$ K$^{-1}$, while the $R = 10a_0$ Cu cluster thermal expansion coefficient is only $\alpha_c^{Cu} = 14.9 \times 10^{-6}$ K$^{-1}$, measured at the center of the cluster. The thermal expansion coefficient for the $R = 10a_0$ Au clusters is $\alpha_c^{Au} = 1.189 \times 10^{-5}$ K$^{-1}$, as compared with $\alpha_p^{Au} = 1.212 \times 10^{-5}$ K$^{-1}$ for a gold single crystal at $P = 0$. In all cases, we find that the thermal expansion coefficient for clusters is smaller than for the zero pressure perfect crystal. This result is counter intuitive since the pressure at the center of the cluster scales linearly with the surface stress (Eq. (2)), which decreases with temperature. This reduction in hydrostatic stress at the center of the cluster would be superimposed upon the thermal expansion of the lattice and hence should result in a larger coefficient of thermal expansion for the clusters. However, this is not the case because the thermal expansion coefficient decreases with increasing compression. This offsets the effect of the reduction in surface stress sufficiently to make the thermal expansion coefficient for the clusters less than that for the zero pressure perfect lattice.

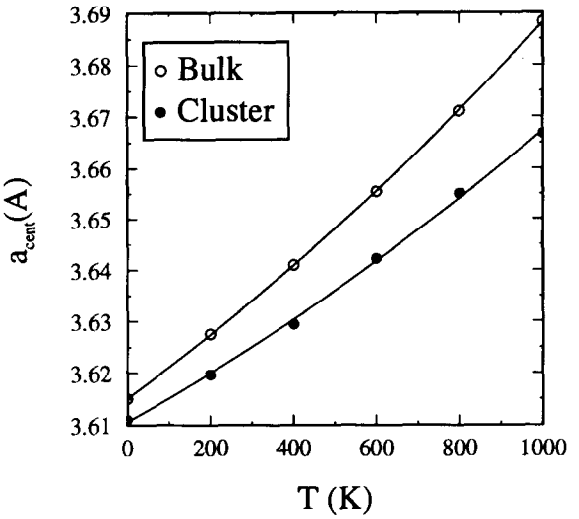


Fig. 11. Variation in the lattice parameter at the center of a Cu cluster of size $10a_0$ and that of bulk Cu with temperature.

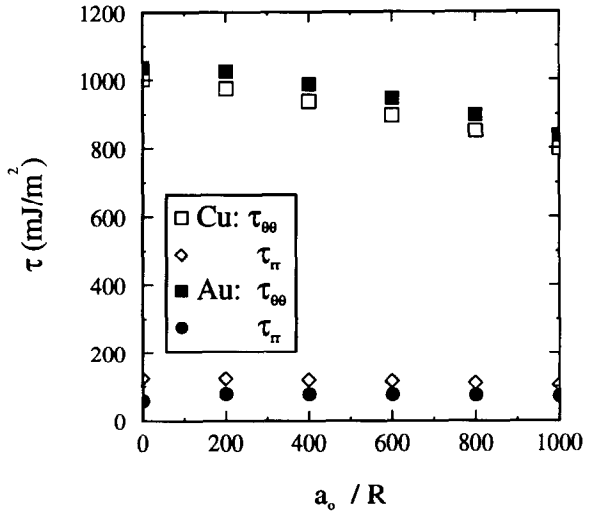


Fig. 10. Variation in surface stress for Au and Cu clusters of size $6a_0$ with temperature. (Cu: (□) $\tau_{\theta\theta}$, (◇) $\tau_{rr}$. Au: (■) $\tau_{\theta\theta}$, (●) $\tau_{rr}$.)

## 4. Discussion

The main cause of the variation of surface properties (free energy, stress, etc.) with cluster size appears to be the discreteness of the lattice planes. Continuous changes in the radius of the "spherical" cluster causes discontinuous changes in the surface structure. Clearly a small change in the radius of the cluster can introduce a new atomic plane, add or remove single adatoms from the surface, etc. These are all purely geometrical effects that are independent of the nature of the atomic bonding. These discontinuous changes in surface structure produce large, discontinuous changes in the surface free energy and surface stress. This was confirmed by normalizing the surface free energy data as a function of cluster radius for the different elements by $\gamma(10a_0)$,

where we found that the cluster size dependence of the average surface energy exhibits a near universal form with only slight deviations between one element and another. These deviations must be attributable to the differences in the interatomic potential from element to element and the resultant variations in the surface relaxations and/or reconstruction.

We have also presented data which shows that the two different methods for determining the surface stresses lead to nearly equivalent results (Fig. 7). This shows the validity of applying simple linear continuum analyses to quantities which otherwise must be determined atomistically. This comparison is unambiguous and works because neither the atomistic nor the continuum determination of the surface stress requires the arbitrary assignment of different atoms of the cluster to bulk and surface regions. The small deviations between the two methods for determining the surface stress is associated with the fact that the cluster is not a true sphere (i.e., it exhibits facets). When the surface normal is not exactly parallel to the radius vector, the identification of the tangential components of the surface stress produces small errors. This causes errors in the surface stress calculation using the method outlined in Eq. (7) and the Appendix. These errors become less important as the cluster increasingly resembles a sphere (i.e., in the large $R$ limit), as shown in Fig. 7.

The identification of the surface thickness is ambiguous since it is sensitive to the definition employed and the physical property that the definition is based upon. Nonetheless, the variation of the stresses within the clusters (Fig. 5) suggest that the surface thickness is approximately $1.5a_0$. This is consistent with other surface studies which show that the surface relaxation decays into the bulk with decay lengths of order a few atomic spacings. We note that the estimate of the surface thickness obtained based upon the spherical clusters may be somewhat high, since the surface has an intrinsic thickness (without relaxations) associated with the discreteness of the atomic planes and the necessity that the surface be curved. In other words, there will always be a surface thickness of at least of order of an atomic

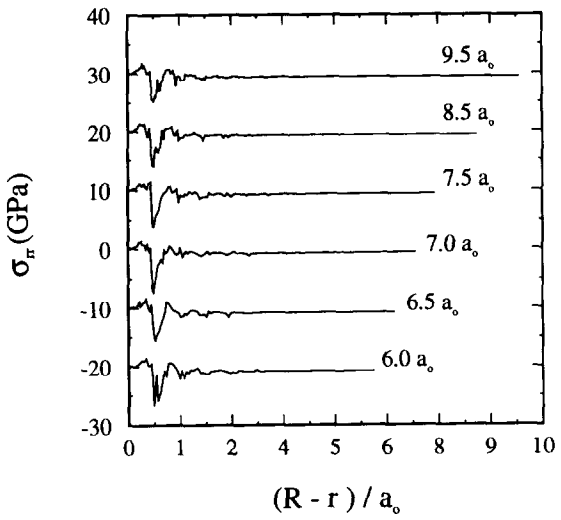


Fig. 12. Variation in internal radial stress of the cluster as a function of scaled distance from the surface, $(R-r)/a_0$, for Au clusters at 400 K. All curves (except for $7a_0$) have been shifted by integral multiples of 10 GPa, for clarity.

spacing due to the geometric necessity of surface steps. We also find that the surface thickness does not change appreciably with temperature (see Fig. 12), again indicating the dominance of local atomic geometry in determining this parameter.

When the clusters become sufficiently large, the variation of average surface energy with cluster size becomes small. In this regime, the average surface energy of the cluster should provide an accurate measure of the average surface energy of a random polycrystalline aggregate. This is based upon the assumptions that the polycrystal is truly untextured and that the grain boundaries intersecting the surface do not play an important role in the polycrystalline average surface properties. Several attempts have been made in the past to correlate this average surface energy with known physical quantities (see the review by Tyson [7]). Most of these methods, however, make assumptions about the structure of the "average" surface and the number of atoms exposed per unit area on such an "average" surface. Since surface properties are often calculated only for high symmetry, low index surfaces, we attempt to

correlate the average surface energy with the energy of these special surfaces.

In order to correlate the average surface properties with those of high symmetry surfaces, we performed a series of atomistic simulations on {100}, {110} and {111} surfaces using essentially the same approach as for the clusters at $T = 0$ K. The surface free energies $\gamma$ are tabulated for these three surfaces and the $R = 15a_0$ clusters of Ag, Au, Cu, and Pt in Table 2. Examination of this table shows that the average surface free energy determined from the cluster is within 1% of the {110} surface energy for Ag, Au, Cu and Pt. The {110} surface is neither the most close packed nor the most commonly occurring facet on the cluster and therefore, the reason for this agreement remains unexplained.

We also fit the average (cluster) surface energy to the {100}, {110} and {111} surface energies using a function of the form

$$\gamma_{\text{cluster}} = \alpha_{\{100\}}\gamma_{\{100\}} + \alpha_{\{110\}}\gamma_{\{110\}} + \alpha_{\{111\}}\gamma_{\{111\}} \quad (8)$$

subject to the constraint that $\Sigma\alpha_i = 1.0$. Only the surface energy data for Ag and Au were used in performing the fit, yielding $\alpha_{\{100\}} = -0.434$, $\alpha_{\{110\}} = 1.249$, $\alpha_{\{111\}} = 0.184$. The results are presented in Table 2 as "Prediction I". If on the other hand, we perform a linear regression on all of the data ($a_{\{100\}} = -0.4013$, $\alpha_{\{110\}} = 1.2095$, $\alpha_{\{111\}} = 0.1954$), the predicted values (Prediction II in Table 2) are in even better agreement with the average cluster values. As expected, based upon the above comparison with the {110} surface, we find a large positive coefficient for {110} (i.e. $\alpha_{\{110\}}$), a small coefficient for {111} (i.e., $\alpha_{\{111\}}$) and a moderately negative coefficient for {100} (i.e., $\alpha_{\{100\}}$). The predicted average surface energy obtained using these values of $\alpha$ in Eq. (8), agrees to within 0.2% with the calculated average (cluster) surface energy for all the elements studied. Therefore, we conclude that a rough approximation of the random polycrystalline surface energy of fcc metals is $\gamma = \gamma_{\{110\}}$, however a better approximation is obtained using a linear combination of the high symmetry surface energies.

While the focus of the present work has been on average surface properties, we can also use the present results to obtain information on high symmetry surfaces. As an example, consider the {110} surface energy. Surface energies of individual surfaces cannot be obtained using such standard methods as the zero creep test. However, since the average cluster surface free energies (in all cases examined herein) are within 1% of the {110} surface energy, an excellent approximation to the {110} surface free energy may be obtained from a zero creep experiment on a random polycrystalline sample. Making use of the correlations between average polycrystalline results and results on individual surfaces (where known) provides a simple method to obtain experimental data without having to resort to single crystals.

Table 2
Values for the surface free energy for the {100}, {110}, {111} surfaces and for the average (cluster) surface free energies of Ag, Au, Cu and Pt for $T = 0$, as well as the results of a linear fit to the {100}, {110} and {111} surface free energies, where only data from the Ag and Au surfaces were used in performing the fit (all values are in mJ/m$^2$)

| | {100} | {110} | {111} | Cluster | Prediction I | Prediction II |
|---|---|---|---|---|---|---|
| Ag | 703 | 765 | 618 | 765 | – | 764 |
| Au | 916 | 978 | 787 | 970 | – | 969 |
| Cu | 1288 | 1412 | 1181 | 1422 | 1423 | 1422 |
| Pt | 1652 | 1755 | 1444 | 1742 | 1742 | 1742 |
| Ni | 1571 | 1720 | 1437 | 1730 | 1731 | 1730 |
| Pd | 1364 | 1478 | 1215 | 1476 | 1479 | 1477 |
| Cu(2) | 1205 | 1323 | 1095 | 1331 | 1332 | 1331 |
| Ni(2) | 1780 | 1943 | 1657 | 1960 | 1961 | 1960 |

The data indicated as Cu(2) and the Ni(2) were obtained using an older version of the EAM potential for these elements [8]. The {100}, {110}, and {111} surface energies for these elements were first published in Ref. [3] for these potentials. The slight discrepancies between the values of these energies in the table and those published in Ref. [3] are attributable to differences in the manner in which the EAM embedding function and its derivatives were calculated.

## 5. Conclusions

We have performed a series of atomistic simulations of nearly spherical, crystalline (fcc) clusters of Ag, Au, Cu and Pt as a function of temperature and cluster size. The focus of the present study was to determine the cluster average surface free energy and cluster average surface stresses with the notion that they provide a measure of the surface properties of random (non-textured) polycrystalline metals. We have used these results to find a simple expression to relate these average surface properties to the oft measured properties of high symmetry/low index surfaces.

We found that atomic clusters with radii greater than approximately $4a_0$ yield cluster average surface energies and surface stresses that are within a few percent of those obtained from clusters of very large size ($15a_0$). It is in the large cluster limit that we expect the cluster average surface properties to be equivalent to the random polycrystalline average surface properties. The variation of the cluster average surface properties with cluster size is dominated by a geometrical effect associated with the discrete spacing between atomic planes and that the differences associated with differences in the atomic bonding between different elements is small, at least for the four elements considered herein. The average surface stress was obtained using an explicit atomistic calculation and by measuring the cluster radius dependence of the pressure internal to the cluster. The two methods yield results in good agreement with each other. Comparison of the cluster averaged surface free energy with those of the more commonly studied high symmetry flat {100}, {110}, and {111} surfaces suggest two useful approximations to the average surface properties. A rough estimate is obtained by simply equating the average surface free energy with the surface free energy of a {110} surface. However, a better estimate is obtained using a linear fit to the {100}, {110}, and the {111} surface free energies. The parameters for use in this fit have been determined. This correlation can be used to obtain the {110} surface energy of fcc crystals from zero-creep experiments on polycrystalline samples.

## 6. Acknowledgments

We would like to thank Professor J. Rickman of Lehigh University for valuable discussions on the topic of this paper. We gratefully acknowledge the support of the Office of Basic Energy Sciences of the United States Department of Energy (Grant No. FG02-88ER-45367), under whose auspices the present research was conducted.

## 7. Appendix. Calculation of stresses on an atom using the EAM potential

In this section we present the expression for the calculation of stresses in a system using EAM potentials and the local harmonic approximation. The total free energy of the system, $A$, can be written as a sum of two parts: a static energy term, $A_0$ (which consists of a pairwise term and an embedding energy term) and a vibrational or dynamic term, $A_v$ (which contributes to both the entropy and the enthalpy).

$$A = A_0 + A_v,$$

$$A_0 = \tfrac{1}{2}\sum_i \sum_{j\neq i} \phi(r^{ij}) + \sum_i F_i(\bar{\rho}_i),$$

$$A_v = \frac{k_B T}{2} \sum_{k=1}^{N} \ln\left( \frac{D^k}{(k_B T)^6} \right). \tag{A.1}$$

In the above equations $\phi(r^{ij})$ is the pairwise energy for atoms $i$ and $j$ and $F_i(\bar{\rho}_i)$ is the embedding energy. $\bar{\rho}_i$ is the total electron density at atom site $i$ and can be written as the sum of the contributions to the electron density at site $i$ from all of the other atoms in the system: i.e. $\bar{\rho}_i = \sum_{j\neq i} \rho(r^{ij})$. $D^k$ is the determinant of the local dynamical matrix, $d^k$, of particle $k$, which for the EAM potential may be written as

$$d^k_{\alpha\beta} = \frac{\partial^2 A_0}{\partial R^k_\alpha \, \partial R^k_\beta}$$

$$= \sum_{l\neq k} \frac{\partial^2}{\partial r^{kl}_\alpha \, \partial r^{kl}_\beta} \phi(r^{kl})$$

$$+ \frac{\partial^2 F_k}{\partial \bar{\rho}^2} \sum_{l\neq k} \frac{\partial}{\partial r^{kl}_\alpha} \rho(r^{kl}) \sum_{l\neq k} \frac{\partial}{\partial r^{kl}_\beta} \rho(r^{kl})$$

$$+\frac{\partial F_k}{\partial \bar{\rho}}\sum_{l\neq k}\frac{\partial^2}{\partial r_\alpha^{kl}\,\partial r_\beta^{kl}}\rho(r^{kl})$$

$$+\sum_{i\neq k}\left(\frac{\partial^2 F_i}{\partial \bar{\rho}^2}\frac{\partial}{\partial r_\alpha^{ki}}\rho(r^{ki})\frac{\partial}{\partial r_\beta^{ki}}\rho(r^{ki})\right)$$

$$+\sum_{i\neq k}\frac{\partial F_i}{\partial \bar{\rho}}\frac{\partial^2}{\partial r_\alpha^{ki}\,\partial r_\beta^{ki}}\rho(r^{ki}). \qquad \text{(A.2)}$$

The stress on any atom $m$ can be written in terms of the derivative of the free energy of the system and the position vectors between the different atoms as

$$\sigma_{\delta\gamma}^m = -\frac{1}{\Omega}\sum_{n\neq m} r_\gamma^{mn}\frac{\partial A}{\partial r_\delta^{mn}}. \qquad \text{(A.3)}$$

$\sigma_{\delta\gamma}^{\mathrm{m}}$ is the $\delta\gamma$ component of the stress on atom $m$, $R_\alpha^i$ is the $\alpha$ co-ordinate of atom $i$ and $r_\gamma^{mn}$ is the $\gamma$ component of the vector $r^{mn}$ between atoms $m$ and $n$. The appropriate derivatives of the free energy in Eq. (A.3) (when EAM potentials are used) are

$$\frac{\partial A_0}{\partial r_\delta^{mn}}$$

$$=\sum_i\sum_{j\neq i}\frac{1}{2}\frac{\partial}{\partial r_\delta^{ij}}\phi(r^{ij})\frac{\partial}{\partial r_\delta^{mn}}r_\delta^{ij}$$

$$+\sum_i\frac{\partial F_i}{\partial \bar{\rho}}\sum_{j\neq i}\frac{\partial}{\partial r_\delta^{mn}}\rho(r^{ij})$$

$$=\frac{\partial}{\partial r_\delta^{mn}}\phi(r^{mn})+\left(\frac{\partial F_m}{\partial \bar{\rho}}+\frac{\partial F_n}{\partial \bar{\rho}}\right)\frac{\partial}{\partial r_\delta^{mn}}\rho(r^{mn}). \qquad \text{(A.4)}$$

$$\frac{\partial A_{\mathrm{v}}}{\partial r_\delta^{mn}} = \frac{k_{\mathrm{B}}T}{2}\sum_{k=1}^{N}\frac{\partial}{\partial r_\delta^{mn}}\ln\left(\frac{D^k}{(k_{\mathrm{B}}T)^6}\right)$$

$$=\frac{k_{\mathrm{B}}T}{2}\sum_{k=1}^{N}\frac{1}{D^k}\frac{\partial}{\partial r_\delta^{mn}}D^k. \qquad \text{(A.5)}$$

$$\frac{\partial}{\partial r_\delta^{mn}}d_{\alpha\beta}^k$$

$$=\sum_{l\neq k}\frac{\partial^3}{\partial r_\delta^{mn}\partial r_\alpha^{kl}\partial r_\beta^{kl}}\phi(r^{kl})$$

$$+\frac{\partial^3 F_k}{\partial \bar{\rho}^3}\sum_{l\neq k}\frac{\partial}{\partial r_\delta^{mn}}\rho(r^{kl})\times\sum_{l\neq k}\frac{\partial}{\partial r_\alpha^{kl}}\rho(r^{kl})\sum_{l\neq k}\frac{\partial}{\partial r_\beta^{kl}}\rho(r^{kl})$$

$$+\frac{\partial^2 F_k}{\partial \bar{\rho}^2}\sum_{l\neq k}\frac{\partial^2}{\partial r_\delta^{mn}\partial r_\alpha^{kl}}\rho(r^{kl})\sum_{l\neq k}\frac{\partial}{\partial r_\beta^{kl}}\rho(r^{kl})$$

$$+\frac{\partial^2 F_k}{\partial \bar{\rho}^2}\sum_{l\neq k}\frac{\partial}{\partial r_\alpha^{kl}}\rho(r^{kl})\sum_{l\neq k}\frac{\partial^2}{\partial r_\delta^{mn}\partial r_\beta^{kl}}\rho(r^{kl})$$

$$+\frac{\partial^2 F_k}{\partial \bar{\rho}^2}\sum_{l\neq k}\frac{\partial}{\partial r_\delta^{mn}}\rho(r^{kl})\sum_{l\neq k}\frac{\partial^2}{\partial r_\alpha^{kl}\partial r_\beta^{kl}}\rho(r^{kl})$$

$$+\frac{\partial F_k}{\partial \bar{\rho}}\sum_{l\neq k}\frac{\partial^3}{\partial r_\delta^{mn}\partial r_\alpha^{kl}\partial r_\beta^{kl}}\rho(r^{kl})$$

$$+\sum_{i\neq k}\left(\frac{\partial^3 F_i}{\partial \bar{\rho}^3}\sum_{j\neq i}\frac{\partial}{\partial r_\delta^{mn}}\rho(r^{ij})\frac{\partial}{\partial r_\alpha^{ki}}\rho(r^{ik})\times\frac{\partial}{\partial r_\beta^{ki}}\rho(r^{ik})\right)$$

$$+\sum_{i\neq k}\left(\frac{\partial^2 F_i}{\partial \bar{\rho}^2}\frac{\partial^2}{\partial r_\delta^{mn}\partial r_\alpha^{ki}}\rho(r^{ik})\frac{\partial}{\partial r_\beta^{ki}}\rho(r^{ik})\right)$$

$$+\sum_{i\neq k}\left(\frac{\partial^2 F_i}{\partial \bar{\rho}^2}\frac{\partial}{\partial r_\alpha^{ki}}\rho(r^{ik})\frac{\partial^2}{\partial r_\delta^{mn}\partial r_\beta^{ki}}\rho(r^{ik})\right)$$

$$+\sum_{i\neq k}\left(\frac{\partial^2 F_i}{\partial \bar{\rho}^2}\sum_{j\neq i}\frac{\partial}{\partial r_\delta^{mn}}\rho(r^{ij})\frac{\partial^2}{\partial r_\alpha^{ki}\partial r_\beta^{ki}}\rho(r^{ik})\right)$$

$$+\sum_{i\neq k}\frac{\partial F_i}{\partial \bar{\rho}}\left(\sum_{l\neq k}\frac{\partial^3}{\partial r_\delta^{mn}\partial r_\alpha^{ki}\partial r_\beta^{ki}}\rho(r^{ik})\right). \qquad \text{(A.6)}$$

The stresses are found by substituting Eqs. (A.4), (A.5) and (A.6) into Eq. (A.3).

## 8. References

[1] C.W. Mays, J.S. Vermaak and D. Kuhlmann-Wilsdorf, Surf. Sci. 12 (1964) 134.
[2] R. Najafabadi, D.J. Srolovitz and R. LeSar, J. Mater. Res. 5 (1990) 2663.
[3] S.M. Foiles, M.I. Baskes and M.S. Daw, Phys. Rev. B 33 (1986) 7983.
[4] R. LeSar, R. Najafabadi and D.J. Srolovitz, Phys. Rev. Lett. 63 (1989) 624.
[5] R. Najafabadi, H.Y. Wang, D.J. Srolovitz and R. LeSar, Acta Metall. Mater. 39 (1991) 3071.
[6] G.J. Ackland and M.W. Finnis, Philos. Mag. A 54 (1986) 301.
[7] W.R. Tyson, Can. Met. Quart. 14 (1975) 307.
[8] S.M. Foiles, Phys. Rev. B 32 (1985) 7685.